

## Magnetization scaling on thick $\text{YBa}_2\text{Cu}_3\text{O}_{7-x}$ single crystals

M. Oussena and P. A. J. de Groot

*Department of Physics, University of Southampton, Southampton, SO9 5NH, United Kingdom*

A. Marshall and J. S. Abell

*School of Metallurgy and Materials, University of Birmingham, Birmingham, B15 2TT, United Kingdom*

(Received 2 August 1993)

Magnetic-hysteresis curves of  $\text{YBa}_2\text{Cu}_3\text{O}_{7-x}$  single crystals are found to exhibit scaling features. The scaling parameters, the full penetration field  $H_p$ , and the associated magnetization  $M_p$ , are determined experimentally as the merging point between the virgin magnetic curve and the  $M$ - $H$  loop envelope. Scaling is performed by dividing  $M$  and  $H$  by  $M_p$  and  $H_p$ , respectively. For magnetic fields higher than  $H_p$ , the  $M$ - $H$  loops, once scaled, lie on a unique envelope, independent of temperature up to the irreversibility line. This result suggests that there is no evidence of any phase transition for  $H > H_p$ . This scaling has been performed on the data obtained for two  $\text{YBa}_2\text{Cu}_3\text{O}_{7-x}$  single crystals, one oxygenated under atmospheric pressure and the other one under high oxygen pressure. The results have shown that pinning in the latter crystal is more effective at intermediate magnetic fields,  $H \sim H_p$ , but less effective at fields  $H$  significantly higher than  $H_p$ .

Although the magnetic properties of  $\text{YBa}_2\text{Cu}_3\text{O}_{7-x}$  (YBCO) single crystals have been widely investigated since the early discovery of the superconducting oxides,<sup>1-3</sup> the behavior with magnetic field and temperature remains to be understood. The shape of the dc magnetic hysteresis loops changes drastically with temperature leading to the possibility of vortex phase transitions. Theoretical calculations have shown that several vortex phase transitions were possible such as glassy phase<sup>4,5</sup> and flux melting phase transitions.<sup>6,7</sup> Since a glassy phase as well as a vortex liquid could be pinned,<sup>8</sup> one could therefore possibly attribute the change in the shape of the magnetic cycles to a transition from a glassy to liquid vortex phase. Recently Krusin-Elbaum *et al.*<sup>9</sup> have related the shape of the magnetization loops to various regimes in the  $H$ - $T$  plane. The crossovers between different regimes were visualized from contours of constant  $J_c$  in the  $H$ - $T$  plane. However, our experimental results show no evidence of any transition for magnetic fields higher than the full penetration field. The results of Krusin-Elbaum *et al.* will be discussed later.

This paper involves an extensive magnetic hysteresis study in two YBCO single crystals taken from the same batch. One of them has been oxygenated under atmospheric pressure (at 450°C for 100 h and then furnace cooled, hereafter called crystal No. 1) and the other one under high oxygen pressure (150 bars at 450°C for 24 h and then furnace cooled, hereafter called crystal No. 2). The experimental results exhibit scaling features. Using the reduced variables  $H/H_p$  and  $M/M_p$ ,  $H_p$  being the full penetration field and  $M_p$  the associated magnetization, one obtains a unique magnetic hysteresis shape, independent of temperature.

The two YBCO crystals used in this investigation were grown from a NaCl:KCl flux, using prereacted and fine-ground YBCO powders as the starting materials.<sup>10-12</sup> Both are heavily twinned with a  $T_c \simeq 91$  K and  $\Delta T_c \simeq 2-3$  K. Crystal No. 1 has a size of about

$3.3 \times 2.4 \times 1.1$  mm<sup>3</sup> and crystal No. 2 was about  $3.8 \times 3.8 \times 0.9$  mm<sup>3</sup>, with the  $c$  axis parallel to the shortest length. The measurements were carried out on an Oxford Instrument vibrating sample magnetometer. Samples were first zero field cooled at the desired temperature (between 10 and 85 K), and then a sweeping magnetic field up to 12 T, at a rate of 20 mT/s, was applied. The magnetic field was first increased from 0 to 12 T and then decreased from 12 to -12 T and finally increased from -12 to 12 T.

Figure 1 shows a set of three  $M$ - $H$  loops (for clarity only half of the loops are represented, the other half can be deduced by symmetry around the origin) at three selected temperatures to emphasize the striking change of the magnetic hysteresis envelope. These curves belong to crystal No. 1. The full penetration field  $H_p$  defined as the first field at which the flux front reaches the center from the surface,<sup>13</sup> is determined experimentally as the field where the virgin magnetic curve and the  $M$ - $H$  loop envelope merge (see Fig. 1). It can be seen that  $H_p$  is quite different from the field at which  $M$  goes through a maximum. At high temperature ( $T > 40$  K), the merging point is less clear because of the increasing depression of the magnetization, that occurs before  $H_p$ , with temperature. This depression gives rise to the well-known fishtail shape. The scaled magnetic loops for the two crystals are represented in Fig. 2. As stated above, scaling is achieved by dividing the magnetic field  $H$  and the magnetization  $M$  by the full penetration field  $H_p$  and the associated magnetization  $M_p$ , respectively. Figure 2(a) corresponds to crystal No. 1 and the solid lines in Fig. 2(b) correspond to crystal No. 2. All the magnetic loops, at different temperatures, once scaled, lie on the same magnetic field envelope for  $H > H_p$ . Figure 2(b) also shows comparison between the two scaled magnetic field envelopes associated to both crystals. For crystal No. 1 (dashed line) pinning seems to be more effective than in crystal No. 2 at fields significantly higher than  $H_p$ . This

situation is reached at high temperatures where the maximum field available (12 T) is much higher than the full penetration field. This result will be discussed later.

To further investigate the above statements, two more experiments on crystal No. 2 have been performed. In the first experiment we have compared the scaled magnetic hysteresis loops at 30, 40, and 50 K (each with a maximum field 12 T) to magnetic hysteresis loops taken at 60 K with different values of maximum field  $H_m$ , such that  $H_m/H_p$  at 60 K was equivalent to the maximum available field (12 T) scaled by the full penetration field  $H_p$  measured at the three lower temperatures. The results are represented in Fig. 3(a). The second experiment consisted of comparing magnetic loops at 50 and 60 K with several reverse legs performed at the same reduced values of  $H_m/H_p$ . One can notice that the scaling is successful at high fields but fails at low fields ( $H < H_p$ , see, for example, the reverse leg of the magnetization curve at 30 K). The results of Figs. 3(a) and 3(b) are in fact predictable from Fig. 2. Indeed, the reverse leg of  $M$ - $H$  loops were parallel. The scaling seems also to break down close to the irreversibility line. Crystal No. 2 [for which pinning seems to be less effective at extreme conditions than crystal No. 1, according to Fig. 2(b)] shows clearly this effect in Fig. 3(c). The latter phenomena could be attributed to the decrease of the pinning as well as to the rapid increase of the relaxation rate with increasing temperature close to the irreversibility line. These relaxation effects are shown to give rise to sweep rate dependence of the hysteresis curves as shown by de Groot *et al.*<sup>14</sup>

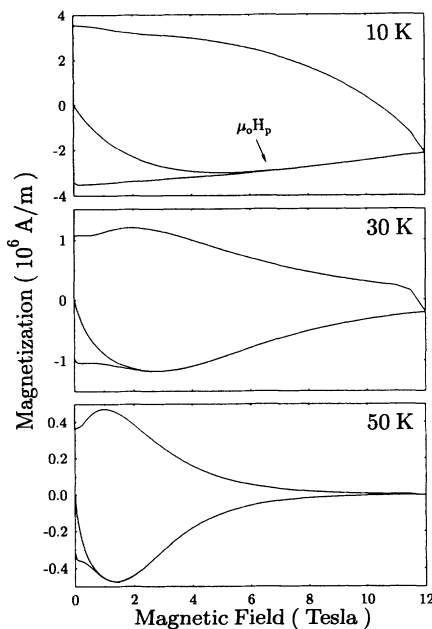


FIG. 1. A set of three magnetic hysteresis loops at three selected temperatures to emphasize the striking change of the shape. These curves belong to crystal No. 1 (oxygenated under atmospheric pressure).  $\mu_0 H_p$  is the full penetration field, determined as the merging point between the virgin magnetic curve and the external envelope.

Figure 4 shows the temperature dependence of  $H_p$  and  $M_p$  for both crystals. For the sake of comparison, the full penetration field  $H_p$  and the associated magnetization  $M_p$  have been normalized to their value at 20 K. These values are, respectively, for crystal No. 1 and No. 2, found to be the following: 5.2 and 11 T for  $\mu_0 H_p$  and 2.15 and 4.8 T for  $\mu_0 M_p$ . At first sight, since  $H_p$  and  $M_p$  do not have the same temperature dependence for the same crystal, it means that the scaling could not be reduced to a one parameter scaling and therefore the Bean model<sup>13</sup> ( $M_p \propto H_p$ ) could not be applied in any case. However, if one consider the low-temperature range ( $T < 50$  K), especially for crystal No. 1 (open squares), one can make the approximation that  $M_p$  and  $H_p$  have the same temperature dependence, consequently  $M_p$  is proportional to  $H_p$  and the scaling could be reduced to one parameter. Figure 4(a) compares the temperature evolution of the normalized full penetration fields  $H_p$  for both crystals. Values deduced for crystal No. 1, which has been oxygenated under atmospheric pressure, decay more rapidly with temperature than those deduced for crystal No. 2, which has been oxygenated under high pressure. This result suggests that pinning is more effective in the latter crystal, for applied magnetic fields of the order of  $H_p$ . Let us go back to the values given

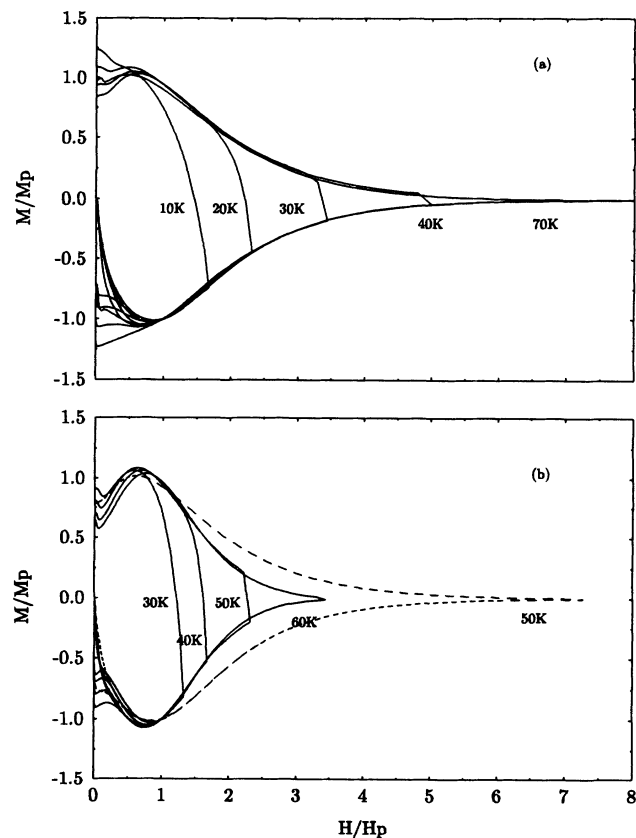


FIG. 2. Scaled magnetization loops, (a) crystal No. 1 (oxygenated under atmospheric pressure) and (b) solid lines, crystal No. 2 (oxygenated under high oxygen pressure). The dashed line in (b) is the scaled magnetic envelope obtained for crystal No. 1. The temperatures indicate the corresponding  $M$ - $H$  loops that have been scaled.

above for  $\mu_0 H_p$  and  $\mu_0 M_p$  at  $T=20$  K. Since these values are size dependent, one has to consider the sample dimensions before any further comparison. If one makes the assumption that the full penetration field  $H_p$  and the associated magnetization  $M_p$  scale with the shortest dimension perpendicular to the applied magnetic field and are related by a proportional factor, as in the Bean model,<sup>13,15</sup> one can correct the values of  $\mu_0 H_p$  ( $T=20$  K) and  $\mu_0 M_p$  ( $T=20$  K) for crystal No. 1 given above, in order to be able to compare them to those of crystal No. 2. The new values are  $\mu_0 H_{pc} = \mu_0 H_p a = 8.2$  T and  $\mu_0 M_{pc} = \mu_0 M_p a = 3.47$  T, where  $a = d_2/d_1$  with  $d_1 = 2.4$  cm and  $d_2 = 3.8$  cm;  $d_1$  and  $d_2$  being the shortest dimensions perpendicular to  $H$  for crystals No. 1 and No. 2, respectively. The corrected values are still lower than those of crystal No. 2 and this result gives further support to the idea that pinning is better for the best oxygenated crystal while dealing with magnetic fields of the order of the full penetration field.

Figure 5 shows a comparison of the critical current density  $J_c$  at  $T=50$  and  $60$  K as a function of the reduced value  $H/H_p$  for both crystals. These temperatures have been chosen to show the behavior of  $J_c$  in a large

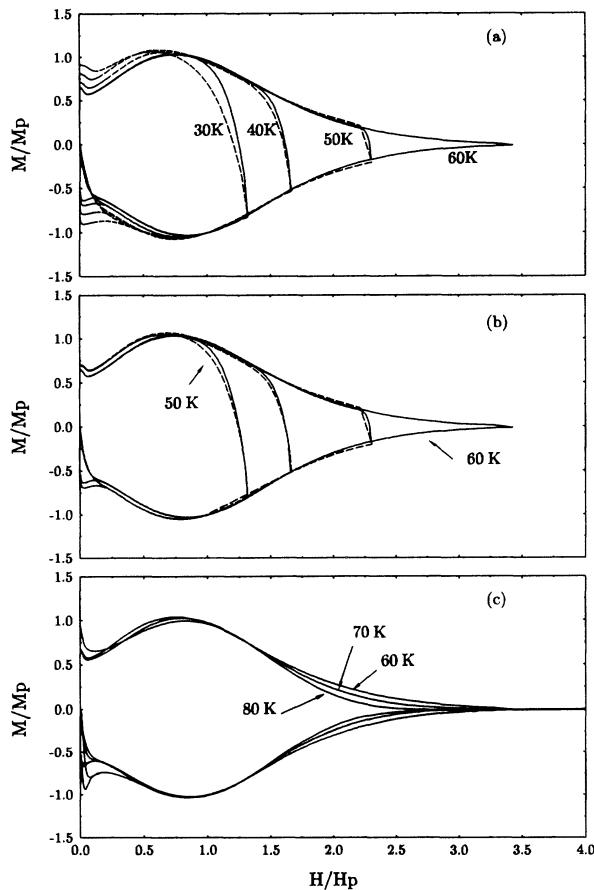


FIG. 3. These curves belong to crystal No. 2. (a)  $M/M_p$  as a function of  $H/H_p$ , dashed lines correspond to the scaled  $M-H$  loops at  $T=30, 40,$  and  $50$  K; solid lines correspond to  $T=60$  K with several reverse magnetic legs. (b) Scaled  $M-H$  loops at  $T=50$  (dashed lines) and  $60$  K (solid lines) with several reverse legs at the same reduced values of  $H/H_p$ . (c)  $M/M_p$  vs  $H/H_p$  for temperatures close to  $T_c$ .

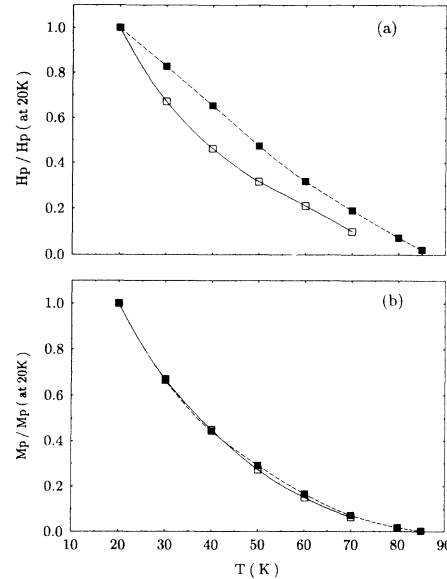


FIG. 4. (a)  $H_p/H_p$  ( $T=20$  K) as a function of  $T$  for crystal No. 1 (open squares) and crystal No. 2 (full squares); (b)  $M_p/M_p$  ( $T=20$  K) vs  $T$  for both crystals, symbols are the same as in (a).

range of values of  $H/H_p$ . The critical current density  $J_c$  is calculated using the formula derived<sup>15</sup> for a square-shaped sample surface with dimensions  $a_x \times a_y$  ( $a_x > a_y$ ):

$$\Delta M = \frac{J_c a_y}{2} \left[ 1 - \frac{a_y}{3a_x} \right] \quad (1)$$

where  $J_c$  is in  $A/m^2$ ,  $a_x$  and  $a_y$  in  $m$ , and finally  $\Delta M$ , the width of the loop, in  $A/m$ .

The results of Fig. 5 support our conclusion concerning pinning for both crystals. It shows clearly that pinning in the well oxygenated crystal (stars) is the most effective for applied magnetic fields,  $H$ , of the order of  $H_p$  and the least effective for  $H$  significantly higher than  $H_p$ .

Similar scaling performed on sintered samples but using the maximum magnetization  $M_m$  and the associated field  $H_m$ , have been reported by Yeshurun *et al.*<sup>16</sup> However, in sintered samples, the full penetration field  $H_p$  is

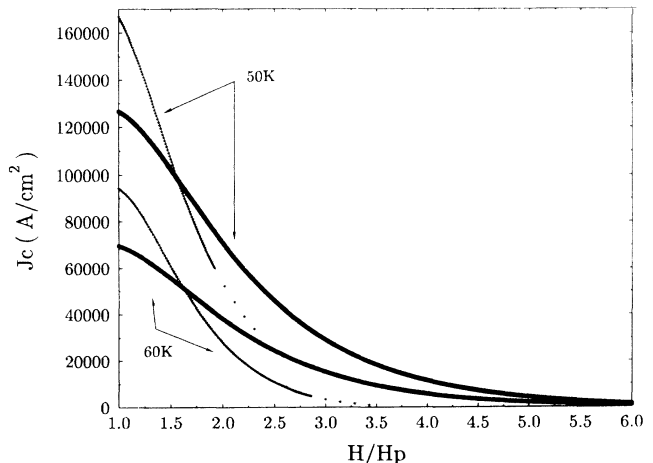


FIG. 5.  $J_c$  vs  $H/H_p$  for crystal No. 1 (solid lines) and crystal No. 2 (stars) at  $T=50$  and  $60$  K.

only slightly different from the field  $H_m$ . One can therefore expect our scaling to be also valid for a sintered material. One of the interesting features of the scaling reported here is that it gives a method to compare the ability of samples, made differently, to carry high-current densities. So far, it has not been clear whether oxygen vacancies increase pinning or reduce it. It has already been reported that vacancies act as pinning centers<sup>17</sup> but recent experimental results on YBCO seemed to contradict this assumption.<sup>18</sup> Actually, in the latter reported results, it is not evident whether the widths of the magnetization loops increase because of the reduction of oxygen vacancies in the same sample after repeated annealing, or simply due to a change of defect structure because of the successive thermal treatments to which the sample was submitted. In our case, if the difference in pinning behavior between the two crystals at applied magnetic fields  $H$  larger than the full penetration field  $H_p$ , could be attributed to oxygen vacancies, then the vacancies would tend to increase the pinning strength rather than reduce it. This behavior could be understood in the framework of the collective pinning theory.<sup>19</sup> In fact, at high field where we believe that the collective pinning theory might apply, the strength of the pinning centers as well as their density are important. According to the collective pinning theory,<sup>19-21</sup> a short-range order in the flux line lattice (FLL) still exists in a volume  $V_c$  called the correlation volume, although pinning destroys the long-range order. If inside this volume there are  $N$  randomly positioned pins, the maximum pinning force exerted on the FLL is equal to  $f_p N^{1/2}$ , where  $f_p$  is the averaged force exerted on the FLL by each pin.

Krusin-Elbaum *et al.*<sup>9</sup> have reported that the shape of the  $M$ - $H$  loops is related to various regimes in the  $H$ - $T$  plane, but our results show no evidence of such a link. It is worth noting that the reported magnetic behavior is quite unusual.<sup>1,22,23</sup> In fact, the ratio of the width over the thickness of their crystal was of the order of 50. This

makes a slab or thin disk geometry with a magnetic field applied perpendicularly, to be a good approximation. In this case Daumling and Larbalestier<sup>24</sup> have shown that the critical state in a thin disk occurs through the thickness  $d$ , not the radius  $r_0$ . Furthermore, the shielding currents create radial fields on the surface of the disk which are of order  $J_c d/2$ . This might affect the shape of the  $M$ - $H$  loops and should be considered in the analysis of the data. Delin *et al.*<sup>25</sup> have investigated thin YBCO crystals similar to those of Krusin-Elbaum *et al.*<sup>9</sup> They have found that the curves could be scaled using a field  $H_b$  and magnetization  $M_b$  originated from a breakpoint in the  $M$ - $H$  loops observed at very high field (for example at  $T=40$  K,  $\mu_0 H_b = 12.5$  T to be compared to  $\mu_0 H_p = 2.4$  T, used in our case for crystal No. 1 which is three times larger than that investigated by Delin *et al.*). In fact, their scaling is not similar to the one reported here, as the experimental definition of the scaling parameters as well as their physical meaning are altogether different.

In conclusion, we have shown that magnetization loops on YBCO single crystals exhibit scaling features. For magnetic fields higher than the full penetration field, the  $M$ - $H$  loops, once scaled, are reduced to a unique envelope, independent of temperature up to the irreversibility line. Our results suggest that there is no evidence of any phase transition or change in the nature of the pinning process for magnetic fields  $H > H_p$ . However, they do not exclude a possible transition for fields lower than  $H_p$ . Our scaling studies have also shown that oxygenating crystals under high oxygen pressure, increases pinning at intermediate fields,  $H \sim H_p$ , but reduce pinning for  $H$  significantly higher than  $H_p$ .

We would thank Dr. G. J. Tomka and Dr. R. Walia for critical reading of manuscript. This research has been supported by the Science and Engineering Research Council.

<sup>1</sup>S. Senoussi, M. Oussena, G. Collin, and I. A. Campbell, Phys. Rev. B **37**, 9792 (1988).

<sup>2</sup>T. R. Dinger, T. K. Worthington, W. J. Gallagher, and R. L. Sandstrom, Phys. Rev. Lett. **58**, 2687 (1987).

<sup>3</sup>S. Senoussi, M. Oussena, C. Aguilon, and P. Tremblay, J. Phys. (Paris) Colloq. **49**, C8-2099 (1988).

<sup>4</sup>M. P. A. Fisher, Phys. Rev. Lett. **62**, 1415 (1989).

<sup>5</sup>D. S. Fisher, M. P. A. Fisher, and D. A. Huse, Phys. Rev. B **43**, 130 (1991).

<sup>6</sup>D. R. Nelson, Phys. Rev. Lett. **60**, 1973 (1988).

<sup>7</sup>A. Houghton, R. A. Pelcovits, and A. Sudbo, Phys. Rev. B **40**, 6763 (1989).

<sup>8</sup>V. M. Vinokur, M. V. Feigel'man, V. B. Geshkenbein, and A. I. Larkin, Phys. Rev. Lett. **65**, 259 (1990).

<sup>9</sup>L. Krusin-Elbaum, L. Civale, V. M. Vinokur, and F. Holtzberg, Phys. Rev. Lett. **69**, 2280 (1992).

<sup>10</sup>J. S. Abell, C. N. N. Darlington, A. Drake, C. A. Hollin, E. M. Forgan, D. A. O'Connor, and S. D. Sutton, Physica C **162-164**, 909 (1989).

<sup>11</sup>A. Drake, J. S. Abell, and S. D. Sutton, J. Less-Common Met. **164-165**, 187 (1990).

<sup>12</sup>F. Gencer and J. S. Abell, J. Cryst. Growth **112**, 337 (1991).

<sup>13</sup>C. P. Bean, Rev. Mod. Phys. **36**, 31 (1964).

<sup>14</sup>P. A. J. de Groot, R. A. Rose, B. Jayaram, G. P. Rapson, and M. Guillot, Supercond. Sci. Technol. **4**, S220 (1991).

<sup>15</sup>R. L. Peterson, J. Appl. Phys. **67**, 6930 (1990).

<sup>16</sup>Y. Yeshurun, A. P. Malozemoff, Y. Wolfus, E. R. Yacoby, I. Felner, and C. C. Tsuei, Physica C **162-164**, 1148 (1989).

<sup>17</sup>M. Daumling *et al.*, Nature (London) **346**, 332 (1990).

<sup>18</sup>M. A. Angadi, Z. X. Shen, and A. D. Caplin, Supercond. Sci. Technol. **5**, S165 (1992).

<sup>19</sup>M. V. Feigel'man, V. B. Geshkenbein, A. I. Larkin, and V. M. Vinokur, Phys. Rev. Lett. **63**, 2303 (1989).

<sup>20</sup>A. I. Larkin and Yu. N. Ovchinnikov, J. Low Temp. Phys. **34**, 409 (1979).

<sup>21</sup>E. H. Brandt, J. Low Temp. Phys. **64**, 375 (1986).

<sup>22</sup>Yanru Ren, P. A. J. de Groot, F. Gencer, and J. S. Abell, Supercond. Sci. Technol. **5**, 349 (1992).

<sup>23</sup>H. W. Weber, Supercond. Sci. Technol. **5**, S19 (1992).

<sup>24</sup>M. Daumling and D. C. Larbalestier, Phys. Rev. B **40**, 9350 (1989).

<sup>25</sup>K. A. Belin, T. P. Orlando, E. J. McNiff, Jr., S. Foner, R. B. van Dover, L. F. Schneemeyer, and J. V. Waszczak, Phys. Rev. B **46**, 11 092 (1992).